Analysing the efficiency of thermopressor application in the charge air cooling system of combustion engine

Dmytro Konovalov[1*], *Roman Radchenko*[1], *Halina Kobalava*[1], *Anatolii Zubarev*[1], *Vyacheslav Sviridov*[1] *and Victoria Kornienko*[1]

[1]Admiral Makarov National University of Shipbuilding, Heroes of Ukraine Avenue, 9, Mykolayiv, 54025, Ukraine.

Abstract. As the analysis of the research results has shown, the use of a thermopressor makes it possible to increase the fuel and energy efficiency of a ship power plant in a wide range of the operation parameters. It can be achieved by cooling the charge air before the engine inlet receiver and by reducing the compression work of the turbocharger. A scheme with the thermopressor application in the cooling system of a low-speed main engine and in the system for utilizing the exhaust gases heat in a heat recovery boiler of one and two pressures was proposed. The use of thermopressors led to a decrease in the compressor power consumption, and therefore in the turbine required power. Therefore, it was appropriate to pass (bypass) the excess amount of gas past the turbine. Accordingly, the thermal potential of exhaust gases was increased. As a result, the temperature of gases at the inlet to the heat recovery boiler was increased by 10-15 °C, and gases heat was increased by 10-15% respectively. The obtained additional steam is advisable to use for driving the utilization turbine generator, thereby reducing the load on the ship's power plant, with a corresponding decrease in fuel consumption of diesel generators by 2-4%.

1 Introduction

Increasing the power of ship power plants based on internal combustion engines was carried out by increasing the flow rate of the working fluid (charge air) and the useful work of combustion products expanding. At the same time, there was a simultaneous reduction in the work for air compressing, which was achieved by cooling air and deep utilization of the combustion products energy. That, in turn, led to a decrease in specific fuel consumption and an increase in efficiency.

2 Literature review

Low-, medium- and high-speed internal combustion engines are widely used in power plants of transport and stationary energy. The air parameters at the turbocharger discharge and at the inlet to the cylinders significantly affect the fuel and energy efficiency of the engine. Every 10 degrees an increase in air temperature causes a decrease in the effective efficiency η_e of marine low-speed diesel engines by 0.5–0.7% [1, 2] with a corresponding increase in specific fuel consumption ge [3]. The decrease in engine power is caused by a decrease in the mass air flow in the cylinders due to a decrease in the air density with an increase in temperature [4, 5].

The development of modern energy efficient technologies for power plants can cause a low level of waste heat use [6, 7]: the temperature of gases after the heat recovery boilers is about 180 °C; charge air temperature is 140–220 °C; the temperature of the engine cylinders cooling water is 90-120 °C. Heat with such a thermal potential can be used in several ways:

1. The use of the combustion products heat for the steam production in the heat recovery boiler (reduction of the specific fuel consumption ge is 2–3%) [8, 9].
2. Turning to heat recovery boilers with two-pressure circuits (additionally increases the capacity of the utilization turbine generator by 15–30%) [10, 11].
3. To improve the turbocharge system [12, 13].
4. The use of the high-temperature cooling method of the internal combustion engine [14].
5. The use of combined energy production technologies with simultaneous production of heat (steam, hot water), electrical energy (generator, shaft generator) and cold (heat-using ejector and absorption refrigeration machines) [15].

The most common way to improve the fuel and energy efficiency of a power plant is contact cooling of the air flow by water injection [16, 17]. It is promising to cool the charge air of the internal combustion engine with a thermopressor which provides an increase in efficiency and a reduction in fuel consumption due to a decrease in temperature and an increase in compressed air pressure. It leads, in turn, to a decrease in the compression power consumption [18]. Changing operating conditions of power plants, and, consequently, the thermal load on the thermopressor, require rational organization of work processes and the determination of a rational design pressure increase that would provide the maximum effect.

* Corresponding author: dimitriyko79@gmail.com

© The Authors, published by EDP Sciences. This is an open access article distributed under the terms of the Creative Commons Attribution License 4.0 (http://creativecommons.org/licenses/by/4.0/).

Thermopressor technologies are based on the implementation of the thermogasdynamic compression effect in special contact heat exchangers (aerothermopressors or thermopressors), which consists in increasing the pressure while decreasing the temperature during the evaporation of a finely dispersed liquid injected into a gas flow moving at a speed close to sound [19, 20].

On the basis of the presented analysis, on the current state of development of technologies for increasing the fuel and energy efficiency of power plants based on internal combustion engines, the main task of the research was formulated: to develop and analyze improved schemes of thermopressor systems for utilizing the energy of combustion products with cooling the working fluid (air) of the engines, principles and methods of their implementation.

3 Research methodology

A comparative-calculation method of research was used in this work to determine the thermodynamic and energy efficiency of a thermopressor cooling system as part of a power plant. A proprietary software package was developed to use this method and it allows: to simulate working processes in a thermopressor; to calculate the main structural elements of the thermopressor; to calculate the energy efficiency and main indicators of the engine when using thermopressor cooling systems, taking into account changes in climatic and hydrometeorological conditions, as well as particular operating modes of the power plant.

The calculation of the thermopressor characteristics (air pressure Pair, air temperature T_{air}, air velocity wair, water velocity w_w, etc.) and its basic geometric parameters of the flow path under specified operating conditions of the power plant engine was carried out according to the indicated methods [21-23]. The calculation took into account the pressure loss in the nozzle (confuser), working chamber, diffuser [24, 25], as well as with the frontal resistance of injected water droplets [26, 27].

The calculation of the main parameters of the internal combustion engine was carried out using the software packages Diesel-RK and CEAS (MAN B&W) [28] taking into account the change in the air parameters at the inlet to the engine cylinders and partial operating modes. To use these software systems, an additional program was developed in which the parameters of wet gas (air) were determined at the inlet and outlet of the turbocharger.

4 Results

A scheme in which the thermopressor is used as a charge air cooler behind a turbocharger of low-speed internal combustion engines with a waste gas heat recovery system in a waste heat recovery boiler is shown in Fig. 1a. The analysis was carried out in relation to the standard traditional scheme for charge air cooling of ship internal combustion engines. The calculations of a low-speed main engine 5S50MC-C (MAN B&W) with a power of N_e = 8300 kW and a speed of n = 105 rpm were carried out. The calculation of the thermopressor parameters was carried out taking into account its joint work with a turbocharger of the pressure-charging system.

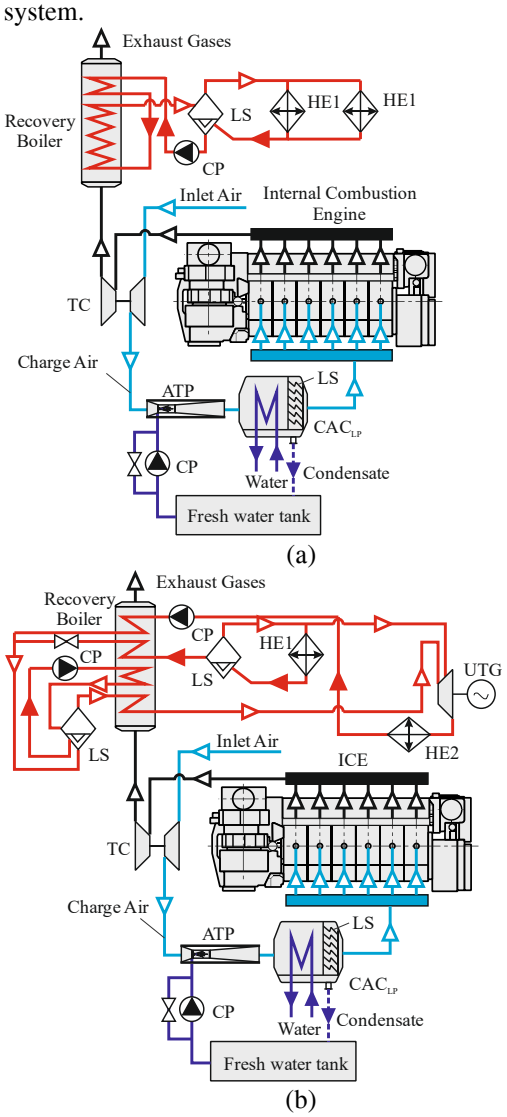

Fig. 1. A scheme of the charge air cooling system with a thermopressor for low-speed marine engines (a); a scheme of a thermopressor charge air cooling system with integrated waste gas heat recovery in the heat recovery boiler and UTG (b): LS – liquid separator; CAC – charge air cooler; TC – turbocharger; ATP –thermopressor.

The increase in pressure in the outlet thermopressor ΔP_{atp} significantly depends on the value of the temperature decrease during cooling Δt_{atp}, and therefore the air temperature at the inlet tatp1 is very important. The temperature in front of the thermopressor corresponds to the discharge air temperature of the turbocharger. In the scheme with one-stage compression, the temperature in front of the thermopressor is t_{c2} = 190–270 °C (Fig. 2a). The temperature behind the turbocharger is the higher, the higher the inlet temperature and the degree of pressure increase in the turbocharger πc. Since the thermopressor cooling system, in fact, is a two-stage air compression (the first stage is a turbocharger, the second stage is a thermopressor), the compression ratio πc of such a scheme will be lower (Fig. 2b), and therefore $t_{c2} = t_{c2}' =$

170–250 °C, that is, the temperature in front of the thermopressor decreases, and accordingly the compression ratio in the air thermopressor πatp will also be lower. Since the required compression ratio for the turbocharger π_c decreases, the compressor work for compression l_c decreases accordingly. For a system with total $\pi_{c.atp}$ = 4.25 the decrease in work is Δl_c = 10–13 kJ/kg; with total $\pi_{c.atp}$ = 4.00 – Δl_c = 9.0–12.5 kJ/kg; with total $\pi_{c.atp}$ = 3.85 – Δl_c = 8.5–12.0 kJ/kg (Fig. 3). Reducing the work on compression l_c allows to reduce the compressor power (Fig. 2b) by ΔN_c = 100–200 kW (10.0–11.5 %), with the same air consumption in the engine.

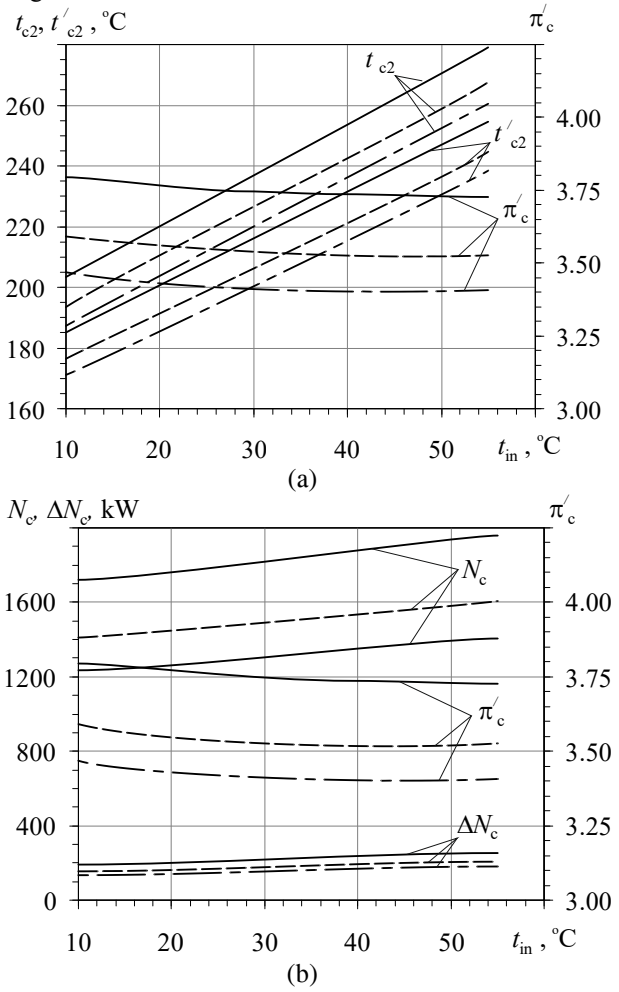

Fig. 2. Dependences of the air temperature at the turbocharger discharge without a thermopressor t_{c2}, by using a thermopressor t_{c2}', degree of pressure increase π_c' (a) turbocharger power N_c, reducing the turbocharger power ΔN_c at different total pressure increase $\pi_{c.atp}$ on the inlet air temperature tin:
_____ – $\pi_{c.atp}$ = 4.25; _ _ _ _ _ – $\pi_{c.atp}$ = 4.00; ___ _ ___ – $\pi_{c.atp}$ = 3.85.

The minimum temperature at the outlet of the thermopressor t_{atp2} was taken to be a temperature 2–3 °C higher than the dew point temperature. It was taken into account that water injection continues in the thermopressor until the air is completely saturated, that is, φ = 100%. The decrease in the air temperature is Δt_{atp} = 110–160 °C, which makes it possible to increase the air pressure after the turbocharger by $\Delta P'_{atp}$ = 520–670 kPa (Fig. 3a) with "ideal" compression (without taking into account friction losses about the channel wall), and with real compression in the thermopressor air pressure increase is ΔP_{atp} = 340–480 kPa, this corresponds to $\Delta P'_{atp}$ = 15–18 % and $\Delta P'_{atp}$ = 10–13% (Fig. 3b).

At the same time, the degree of decrease in air temperature in the thermopressor was T_{atp1}/T_{atp2} = 1.30–1.45. The thermopressor is the second stage of compression in the pressure-charging system; accordingly, it is appropriate to evaluate its efficiency by the degree of pressure increase π_{atp} = 1.10–1.13.

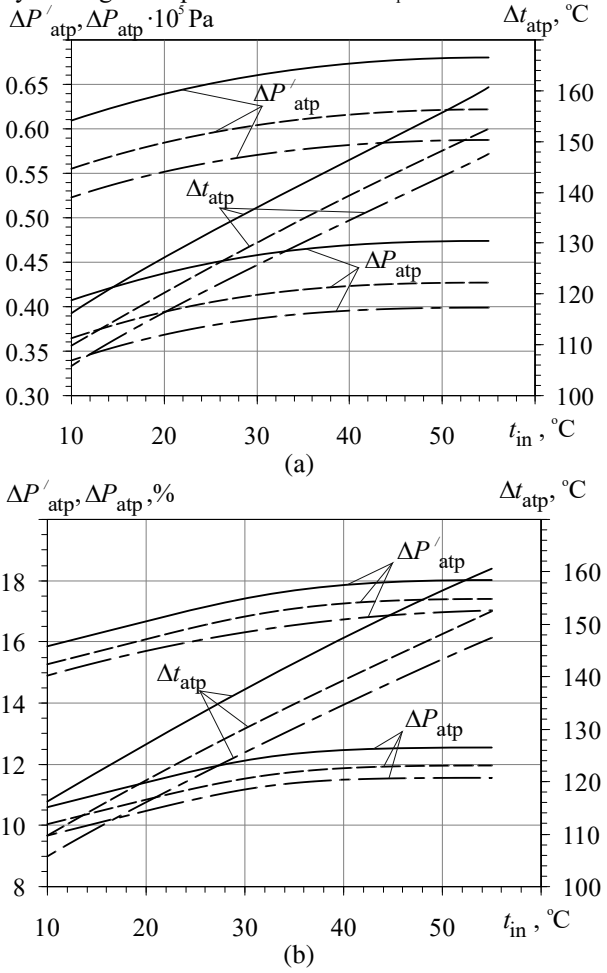

Fig. 3. Dependences of the decrease in the thermopressor air temperature Δt_{atp}, an increase in the air pressure at the discharge with "ideal" compression $\Delta P'_{atp}$, with real compression ΔP_{atp} (a, b) at different total pressure increase $\pi_{c.atp}$ on the inlet air temperature tin:
_____ – $\pi_{c.atp}$ = 4.25; _ _ _ _ _ – $\pi_{c.atp}$ = 4.00; ___ _ ___ – $\pi_{c.atp}$ = 3.85.

A decrease in air temperature and an increase in pressure in the thermopressor are quite significant, which affects the decrease in flow rates in the turbocharger, as a result, the exhaust gases temperature of the utilization turbine (UT) increases (Fig. 4a). Thus, at a constant temperature of gases at the UT inlet (t_{g1} = 300–400 °C), the temperature of the exhaust gases is t_{g2} = 205–285 °C, in the scheme by using the thermopressor the temperature of the exhaust gases is t_{g2} = 220–300 °C, which is 15 °C higher for the basic version.

Comparison of the thermopressor with the heat exchanger, from the point of view of the heat exchanger (charge air cooler), shows that the heat load on the thermopressor is Q_{atp} = 1600–3700 kW (Fig. 4b).

However, the air temperature at the discharge of the thermopressor is still high and amounts to t_{atp} = 65–85 °C. Therefore, it is advisable to install an additional heat exchanger behind the thermopressor. The heat load on such charge air cooler is Q_{cac2} = 200–1200 kW, hence the total heat load on the thermopressor and the additional heat exchanger is Q_{t2} = 2000–4800 kW, which is less than for the standard charge air cooling system Q_{st2} = 2400–5200 kW (7–15 %). The increase in the thermal load on the standard charge air cooler can be explained by reducing the air temperature in the turbocharger with the thermopressor at 20–25 °C.

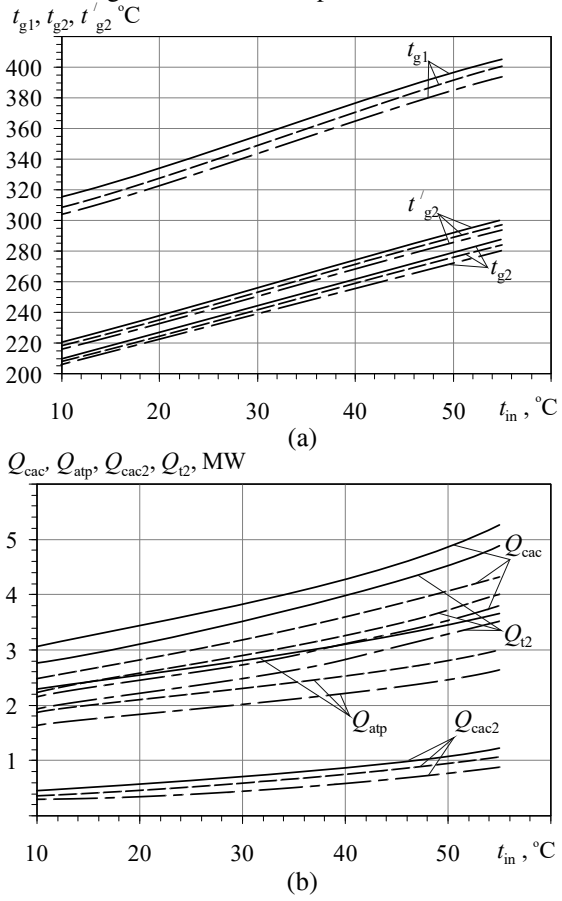

Fig. 4. Dependences of the exhaust gases temperature before UT t_{g1}, exhaust gases temperature UT (for a circuit without a thermopressor) t_{g2}, exhaust gases temperature UT (for a circuit with a thermopressor) t'_{g2} (a), heat load on: heat exchanger Q_{cac}, for thermopressor Qatp, for additional heat exchanger Q_{cac2}, total heat load Q_{t2} (b) at different total pressure increase $\pi_{c.atp}$ on the inlet air temperature tin:
_____ – $\pi_{c.atp}$ = 4.25; _ _ _ _ _ – $\pi_{c.atp}$ = 4.00; ___ _ ___ – $\pi_{c.atp}$ = 3.85.

The efficiency of thermopressor operation was estimated taking into account the energy consumption for the supply of fresh water for injection in the thermopressor nozzle. According to calculations, the water consumption for injection into the thermopressor is G_w = 0.6–1.2 kg/s, while the pump drive power is N_w = 0.3–0.7 kW. The moisture content of the air increases by Δd_{atp} = 40–60 g/kg. The injection pump power is rather small (0.3–0.5%) compared to the decrease in the compressor power ΔN_c = 100–200 kW.

The use of the thermopressor leads to a decrease in the turbocharger power, and then the unnecessary heat drop (work) of the TC turbine decreases, the required power of the turbine and the required gas flow rate decrease. Hence, it is appropriate to pass the excess amount of gas past the turbine, due to which the exhaust gases temperature in front of the heat recovery boiler increases. Hence, the thermal potential of waste gases increases, which can be used in a waste heat recovery boiler. So the temperature at the heat recovery boiler inlet grows by almost Δt_{rb} = 10–15 °C, taking into account the temperature of the gases at the heat recovery boiler outlet is constant and equal to t_{rb2} = 160 ° C, the additional heat load (with the corresponding additional consumption steam) is ΔQ_{rb} = 150–300 kW (10-15%).

As shown by the calculations of the thermal scheme, the amount of steam generated in the heat recovery boiler is more than enough to meet the needs of this dry cargo ship. So, it is advisable to use the obtained additional steam to drive a utilization turbine generator (UTG), thereby reducing the load on the ship's power plant, with a corresponding decrease in fuel consumption for diesel generators.

A scheme of the thermopressor charge air cooling system with integrated heat recovery from exhaust gases in the heat recovery boiler with two pressure circuits and UTG is shown in Fig. 1b. Analysis of the UTG operation shows (Fig. 5) that an increase in heat power in a waste heat recovery boiler of two pressures allows an increase in steam production by ΔD_{utg} = 0.07–0.12 kg/s (250–430 kg/h), which increases the power of UTG by ΔN_{utg} = 45–90 kW (6–10% of the rated power of the UTG).
When two MAN B&W 7L16/24 diesel generators are installed on board with a rated power N_e = 770 kW and a specific fuel consumption g_e = 195 g/(kW·h), a decrease in the load on the ship's power plant when the UTG is turned on (Fig. 5) reduces the specific fuel

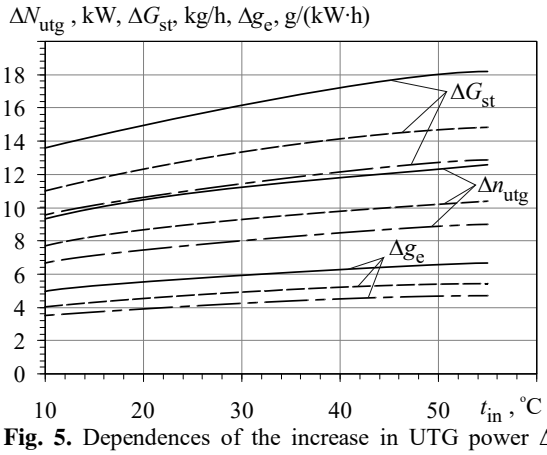

Fig. 5. Dependences of the increase in UTG power ΔN_{utg}, reduction in fuel consumption ΔG_{st}, reduces the specific fuel consumption Δg_e at different total pressure increase $\pi_{c.atp}$ on the inlet air temperature tin:
_____ – $\pi_{c.atp}$ = 4.25; _ _ _ _ _ – $\pi_{c.atp}$ = 4.00; ___ _ ___ – $\pi_{c.atp}$ = 3.85.

consumption by Δg_e = 4–7 g/(kW·h), with a temporary reduction in fuel consumption ΔG_{st} = 10–18 kg/h (240–430 kg/day). The analysis of economic feasibility shows that the reduction in fuel consumption per voyage within 28 days will be ΔG_v = 7–12 tons. Taking into account the summer operation of the vessel, the reduction in fuel consumption per year will be ΔG_{year} = 90–150 tons.

5 Conclusion

The analysis of circuit solutions to use the thermopressor technologies for charge air cooling of engines is studied. It showed that the load reduction on the ship power plant with a corresponding reduction in the fuel consumption of diesel generators is 2–4%. In this case, the production of an additional amount of steam by 10–15% can be ensured.

The branches of the predominant application of thermopressor technologies include plants of stationary and marine power energy based on internal combustion engines and gas turbine engines. The use of thermopressor technologies provides a significant reduction in fuel consumption and can contribute to an increase in the energy security level of the state.

References

1. Z. Yao, Z. Q. Qian, R. Li, E. Hu. Energy efficiency analysis of marine high-powered medium-speed diesel engine base on energy balance and exergy. Energy, 2019, 991-1006.
2. A. Radchenko, E. Trushliakov, K. Kosowski, D. Mikielewicz, M. Radchenko. Innovative turbine intake air cooling systems and their rational designing. Energies, 2020, 13(23), 6201. doi:10.3390/en13236201.
3. N. Bistrovic, D. Bernecic. Energy efficiency in maritime transport. 18th Annual General Assembly of the International Association of Maritime Universities – Global Perspectives in MET: Towards Sustainable, Green and Integrated Maritime Transport, IAMU, Vol. 32017, 2017, 47-50.
4. E. Trushliakov, A. Radchenko, M. Radchenko, S. Kantor, O. Zielikov. The Efficiency of Refrigeration Capacity Regulation in the Ambient Air Conditioning Systems In: Ivanov V., et al. (eds.) Advances in Design, Simulation and Manufacturing III. LNME, 2000. 343-353. doi: 10.1007/978-3-030-50491-5_33.
5. F. Baldi, F. Ahlgren, T.V. Nguyen, M. Thern, K. Andersson. Energy and exergy analysis of a cruise ship. Energies, Vol. 11, No. 10, 2018.
6. A.A. Manzela, S.M. Hanriot, L.C. Gomez, J.R. Sodre. Using engine exhaust gas as energy source for an absorption refrigeration system. Appl. Energy, Vol. 8, 2010, 1141-1148.
7. D. Steffens. The Diesel Engine and the Environment. Session Chair - Wayne Cole, Houston, Texas: Cole Engineering, 2003, p. 36.
8. Diesel Engines for Independent Power Producers and Captive Power Plants. MAN-Burmeister & Wain Diesel A/S: Copenhagen, Denmark, 2001, 352-399.
9. Project Guide Two-stroke Engines. MC Programme. Copenhagen, Vol. 1, 1986.
10. K. Danilecki, J. Eliasz. The Potential of Exhaust Waste Heat Use in a Turbocharged Diesel Engine for Charge Air Cooling. SAE Technical Paper 2020-01-2089, 2020.
11. R. Cipollone, D. Di Battista, D. Vittorini. Experimental assessment of engine charge air cooling by a refrigeration unit. Energy Procedia, 2017, 1067-1074.
12. L. Guzzella, A. Amstutz. Control of diesel engines. IEEE Control Systems, Vol. 18(5), 1998, 53-71. doi:10.1109/37.722253.
13. A.G. Stefanopoulou, I. Kolmanovsky, J.S. Freudenberg: Control of variable geometry turbocharged diesel engines for reduced emissions. IEEE Transactions on Control Systems Technology, Vol. 8(4), 2000, 733-745.
14. M. Radchenko, R. Radchenko, V. Tkachenko, S. Kantor, E. Smolyanoy. Increasing the Operation Efficiency of Railway Air Conditioning System on the Base of Its Simulation Along the Route Line. In: Nechyporuk M., Pavlikov V., Kritskiy D. (eds) Integrated Computer Technologies in Mechanical Engineering. AISC, 2020, vol 1113. Springer, Cham, 461-467. doi.org/10.1007/978-3-030-37618-5_39.
15. V. Kornienko, R. Radchenko, D. Konovalov, A. Andreev, M. Pyrysunko Characteristics of the Rotary Cup Atomizer Used as Afterburning Installation in Exhaust Gas Boiler Flue In: Ivanov V., et al. (eds.) Advances in Design, Simulation and Manufacturing III. LNME, 2000. 302-311. doi: 10.1007/978-3-030-50491-5_29.
16. M. Jonsson, J. Yan. Humidified gas turbines – a review of proposed and implemented cycles. Energy, No. 30, 2005, 1013-1078.
17. W.R. Sexton, M.R. Sexton. The Effects of Wet Compression on Gas Turbine Engine Operating Performance. Proceedings of GT2003 ASME Turbo Expo: Power for Land, Sea and Air 2009, Atlanta, Georgia, USA, 2009. doi: 10.1115/GT2003-38045.
18. D. Konovalov, H. Kobalava, V. Maksymov, R. Radchenko, M. Avdeev. Experimental research of the excessive water injection effect on resistances in the flow part of a low-flow aerothermopressor. In: Ivanov V., et al. (eds.) Advances in Design, Simulation and Manufacturing III. LNME, 2000, 292-301. doi: 10.1007/978-3-030-50491-5_28.
19. A. Fowle. An experimental investigation of an aerothermopressor having a gas flow capacity of 25 pounds per second. Massachusetts Institute of Technology, USA, 1972.
20. A.H. Shapiro, K.R. Wadleigh: The Aerothermopressor – a Device for Improving the Performance of a Gas-Turbine Power Plant. Proceedings of the Trans. ASME, Cambridge, USA, 1956, 617-653.
21. D. Konovalov, H. Kobalava, M. Radchenko, I.C. Scurtu, R. Radchenko. Determination of hydraulic resistance of the aerothermopressor for gas turbine cyclic air cooling. In: TE-RE-RD 2020, E3S Web of Conferences 180, 01012, 2020, 14 p.

22. D. Konovalov, H. Kobalava, M. Radchenko, V. Sviridov, I.C. Scurtu. Optimal Sizing of the Evaporation Chamber in the Low-Flow Aerothermopressor for a Combustion Engine. Advanced Manufacturing Processes II. InterPartner 2020. LNME, 2021, 654-663. doi: 10.1007/978-3-030-68014-5_63.
23. H.W. Oh. Advanced Fluid Dynamics. Rijeka, Croatia, 2012, 282 p.
24. S.K. Wang. Handbook of air conditioning and refrigeration, Second Edition ed., McGraw-Hill, 2000, 1401 p.
25. L. Bohdal, L. Kukielka, S. Świłło, A. Radchenko, A. Kułakowska. Modelling and experimental analysis of shear-slitting process of light metal alloys using FEM, SPH and vision-based methods. AIP Conference Proceedings 2078, 020060, 2019, doi: 10.1063/1.5092063.
26. K.G. Chandra, D.D. Kale. Pressure drop for two-phase air-non-newtonian liquid flow in static mixers. The Chemical Engineering Journal and The Biochemical Engineering Journal, V. 59, No. 3, 1995, 277-280.
27. L. Bohdal, L. Kukielka, A. Radchenko, R. Patyk, M. Kułakowski, J. Chodór. Modelling of guillotining process of grain oriented silicon steel using FEM. AIP Conference Proceedings 2078, 020080, 2019, doi: 10.1063/1.5092083.
28. CEAS Engine Calculations. MAN Diesel Turbo. URL: https://marine.man-es.com/two-stroke/ceas.